Design of Gate System in Injection Molding of a Dashboard by CAMP*mold*

D. S. Choi*, K. H. Han**, H. S. Kim***, and Y. T. Im*

Key Words : Injection Molding, CAMP*mold*, Gate Location, Dummy Runner

Abstract

Injection molding is widely used in producing various plastic parts due to its high productivity and the demand for high precision injection molded products is ever increasing. To achieve successful product quality and precision, the design of gating and runner systems in the injection mold is very important since it directly influences melt flow into the cavity. Some defects such as weld lines and overpacking can be effectively controlled with proper selection of gate locations. In the present study, the design of gate locations in injection molding of a dashboard for automobiles was carried out with CAMP*mold*, a PC-based simulation system for injection molding. A dummy runner was developed to simulate a runner system in order to increase the efficiency of the analysis. The numbers and locations of gates were varied in the present investigation as that an acceptable design was obtained in terms of reduced maximum pressure and clamping force.

1. Introduction

Injection molding is a manufacturing process by which complex parts can be produced quickly in large quantities. Product quality depends on the material used, mold design, and processing conditions. The overall mold design must consider the cavity, gate and runner systems, and cooling system[1-4].

Gating design is composed of the selection of the number, type, and allocation of gates[1]. Gate allocation is one of the most important design tasks in mold design. Gate location affects the filling time, temperature, and pressure distributions since it controls the balance and direction of polymer flow. Improper gate locations can cause overpacking, high shear stress, poor welds, and excessive warpage. To reduce these defects, gate must be located such that the polymer reaches the edges of the cavity at almost the same time.

Runner design is a two stage process. First, configuration design involved with constructing the runner layout is determined to carry plastic melt from the machine nozzle to various cavities. Second, in parametric design, the diameters of the runner elements and gates are estimated so as to completely fill the cavities[1].

Configuration design involves determination of the number of cavities, generation of local configurations, and selection of a global configuration. The local configuration is the part of a runner system that connects an entrance point to the gates in a part, while the global configuration connects the tip of the

* Department of mechanical engineering, KAIST
** Hyundai motor company
*** School of automotive, industrial and mechanical engineering, Daegu university

nozzle to the entrance points of the various local configurations.

In parametric design, the flow-paths are balanced by sizing the runner elements and gates such that all the cavities will be filled at the same time and have the same pressure drop.

For the design of gate locations, a runner system must be included in the simulation to supply polymer to all gates. In this study, a dummy runner system was developed to numerically imitate the runner system. This was included in CAMP*mold*(5-6), a PC based simulation program for injection molding, to design gate locations for a dashboard molding example.

The main objective of this design of gate locations is to minimize the injection pressure and clamping force and to remove weld lines. Several simulations with varying number of gates and gate locations were carried out.

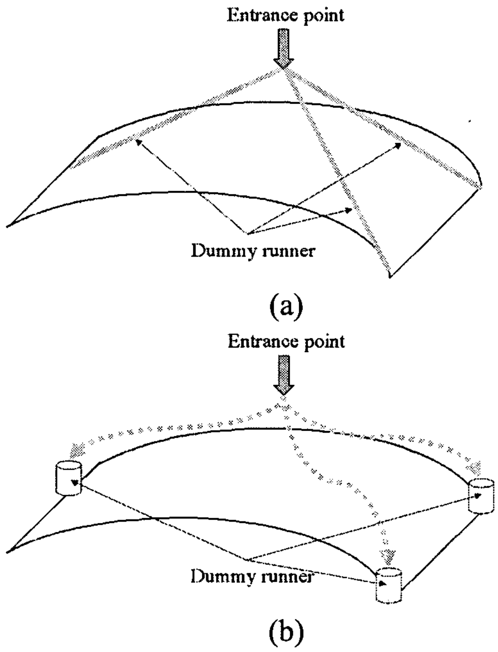

Fig. 1 Schematic diagram of dummy runners.

2. Dummy runner

CAMP*mold* is a simulation system for injection molding that can analyze temperature and pressure distributions, warpage of the final part(7), and fiber orientation in short fiber reinforced injection molding(8-10). And as mentioned, it offers a dummy runner system for user convenience(11).

The dummy runner system was developed to divide polymer inflow from the entrance to each gate. The polymer must not undergo any cooling during this process. For this, the time for the polymer to pass the dummy runner must be very small. This can be realized by assuming the length of a dummy runner to be negligible and the radius to be very large. This is impossible practically but it is assumed numerically.

In the simulation of multigate systems, each gate can be connected to one point with dummy runners and that point is set to be the entrance point. As can be seen in Fig. 1 (a), the lengths of dummy runners are different from each other geometrically, but they are recognized as having the same length in numerical calculations as shown in Fig. 1 (b). Therefore, each flow front will reach its gate at the same time.

3. Design of Gate Location in Injection Molding of a Dashboard

Dashboard is an automobile part that is manufactured by injection molding. The proper design of gate locations for a dashboard is particularly important because of the possibility of short shots due to its large size.

A dashboard, 80 cm wide and 5 mm in thickness, is shown in Fig. 2. For numerical modeling, 3506 elements and 1933 nodes were used. To describe the shear thinning effect, a Cross-type model(12) was employed and for accurate modeling of density, the Tait state equation(13) was used. The material was PS (polystyrene) and the material values used in the numerical simulation are listed in Tables 1 and 2.

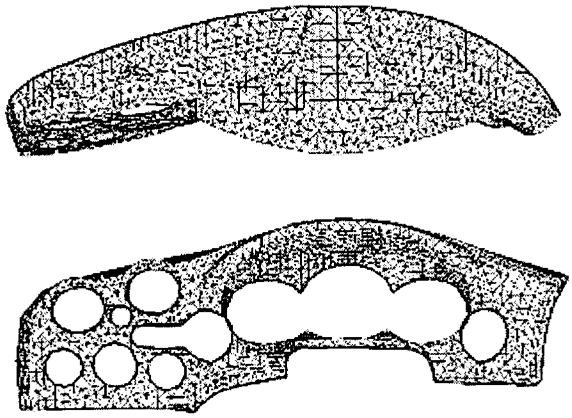

Fig. 2 Mesh layout for the dashboard panel.

The melt temperature was 230 °C, the mold temperature 50 °C, and the injection rate 300 cm^3/s.

The objective of the design of gate locations was as follows: First, minimize maximum filling pressure. If high pressure is required for polymer filling, some defects such as short shots can occur. Second, minimize the clamping force. In most cases, low filling pressure leads to low clamping force but not always. Third, remove or reduce weld lines.

Table 1 Viscosity model constants for PS.

Symbol	Value
n	0.2520
τ^*	3.080×10^{4} Pa
D_1	4.76×10^{10} Pa·s
D_2	100 °C
D_3	5.1×10^{-7} °C/Pa
A_1	25.74
A_2	61.06 °C

$$\eta(\dot{\gamma},T,p)=\frac{\eta_0(T,p)}{1+\left\{\frac{\eta_0(T,p)\dot{\gamma}}{\tau^*}\right\}^{1-n}},$$

$$\eta_0(T,p)=D_1\exp\left\{-\frac{A_1[T-T^*(p)]}{A_2+D_3p+[T-T^*(p)]}\right\},$$

$$T^*(p)=D_2+D_3p.$$

Table 2 Specific-volume model constants for PS.

Symbol	Value
$b_{1,l}$	9.72×10^{-4} m^3/kg
$b_{2,l}$	5.44×10^{-7} $m^3/kg°C$
$b_{3,l}$	1.68×10^{8} Pa
$b_{4,l}$	4.08×10^{-3} $°C^{-1}$
$b_{1,s}$	9.72×10^{-4} m^3/kg
$b_{2,s}$	2.24×10^{-7} $m^3/kg°C$
$b_{3,s}$	2.62×10^{8} Pa
$b_{4,s}$	3.00×10^{-3} $°C^{-1}$
b_5	100 °C
b_6	5.1×10^{-7} °C/Pa

$$v(T,p)=\frac{1}{\rho}=v_0(T)\left[1-0.0894\ln\left(1+\frac{p}{B(T)}\right)\right],$$

$$v_0(T)=\begin{cases} b_{1,l}+b_{2,l}(T-b_5) & \text{for } T>T_g \\ b_{1,s}+b_{2,s}(T-b_5) & \text{for } T\le T_g \end{cases},$$

$$B(T)=\begin{cases} b_{3,l}\exp\{-b_{4,l}(T-b_5)\} & \text{for } T>T_g \\ b_{3,s}\exp\{-b_{4,s}(T-b_5)\} & \text{for } T\le T_g \end{cases},$$

$$T_g(p)=b_5+b_6p.$$

With such objectives, numerous simulations with varying number of gates (1-3) and various gate locations were carried out. The results are given in the following depending on the number of gates used.

(i) 1 gate

Three cases as shown in Fig. 3 were simulated and compared to determine the best gate location. Fig. 4 shows the filling time distribution for each case and Table 3 lists the maximum pressure and clamping force for each case. The maximum pressure is always located at the entrance point.

For cases 1 and 2, the finally filled regions were located to the left and to the right, respectively. Such filling patterns led to high maximum pressure and clamping force. In comparison, the polymer flow was more balanced in case 3 such that the maximum pressure and clamping were relatively lower.

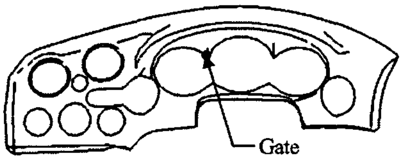

Case 1

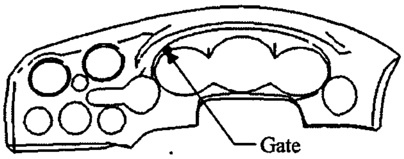

Case 2

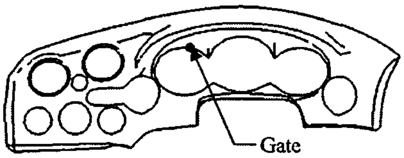

Case 3

Fig. 3 Three gate location cases using a single gate.

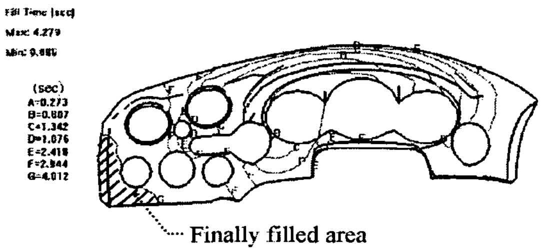

Case 1

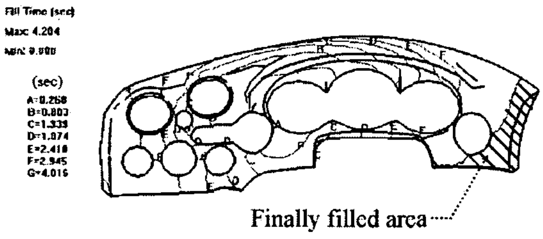

Case 2

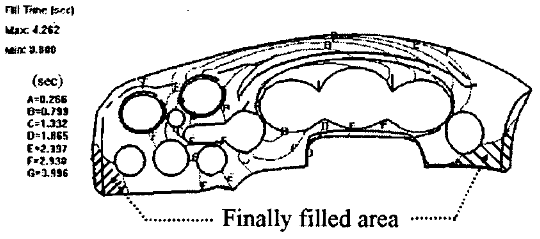

Case 3

Fig. 4 Filling time distribution for each case using a single gate.

Table 3 Maximum pressure and clamping force for each case.

	Case 1	Case 2	Case 3
P_{max} (MPa)	38.44	36.15	28.45
F_{clamp} (kN)	1870.68	1845.37	1070.95

(ii) 2 gates

Fig. 5 shows a case in which 2 gates were scattered to the right and left. This resulted in 20.24 MPa maximum pressure and 1228.09 kN clamping force. The maximum pressure was lower than that of using only a single gate, but the clamping force was higher. This was because the normal vector of the region where high pressure existed was inline with the clamping direction. In this case, a weld line was formed in middle of the part as shown in Fig. 6. To remove this weld line, four candidates as shown in Fig. 7 were examined. Table 4 lists the maximum pressure and clamping forces for each case.

Case 1 gave the best result but it was worse than that of using just a single gate. This was because the two gates shown in Fig. 7 were all allocated near the center region, such that the balance of polymer flow was less effective than that of using a single gate.

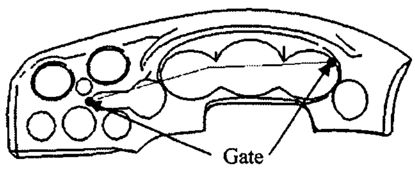

Fig. 5 Simulation example using two gates.

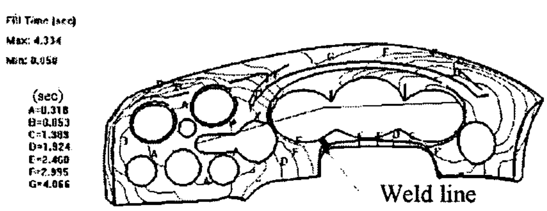

Fig. 6 Filling time distribution and weld line formation when using two gates.

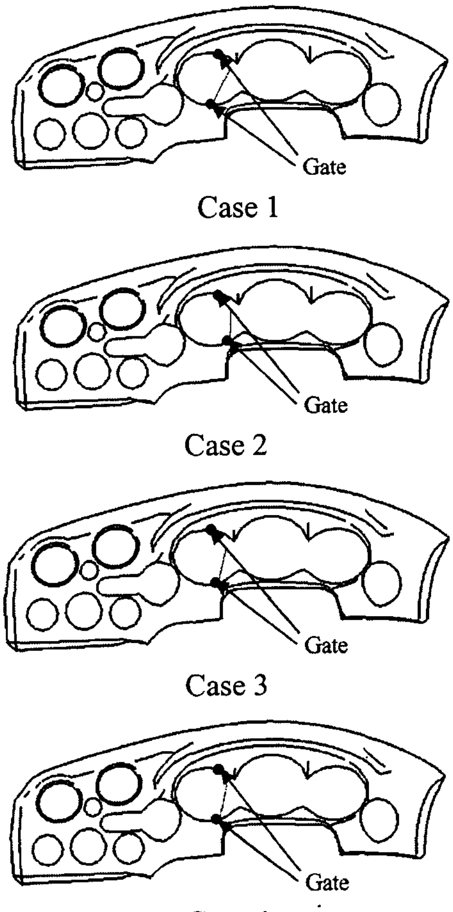

Fig. 7 Four gate location cases using two gates.

(iii) 3 gates

Fig. 8 shows four candidates of gate locations using three gates. Two gates were scattered to the left and right to decrease pressure and the remaining gate was positioned to remove weld lines.

Table 4 Maximum pressure and clamping force for each case using two gates.

	Case 1	Case 2	Case 3	Case 4
P_{max} (MPa)	28.89	33.38	31.64	32.33
F_{clamp} (kN)	1366.36	1779.68	1608.22	1710.34

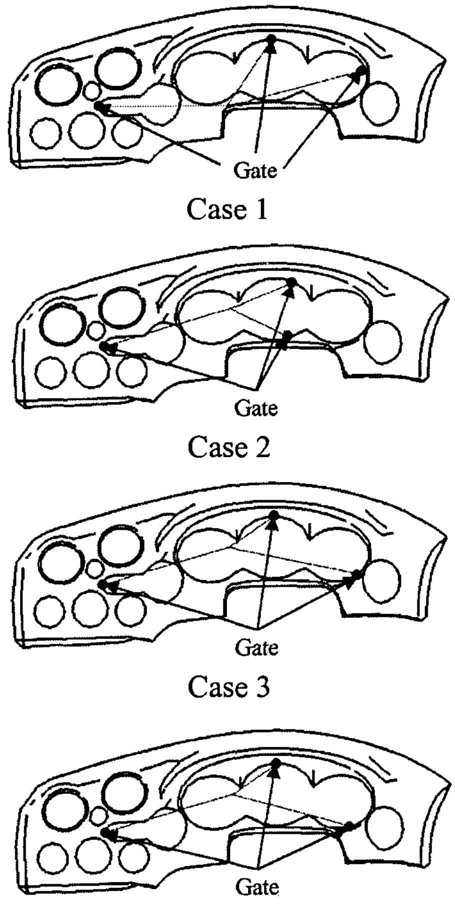

Fig. 8 Four gate location cases using three gates.

As can be seen in Fig. 9, all four cases failed to completely remove the weld line. In case 1 two flow fronts with relatively low temperature (130~140°C) joined at a small meeting angle. In the other cases, the flow fronts joined at relatively higher temperatures (140~150°C) at large meeting angles. This decreased the size of the weld line[(14)]. In particular, it was expected that the weld line in case 2 would be very small or negligible.

Table 5 lists the maximum pressure and clamping force for each case. It can be seen that the maximum pressure and the clamping force was the lowest for case 3. However the size of the weld line was the smallest in case 2. Therefore the best gate locations could be selected somewhere between cases 2 and 3.

Table 5 Maximum pressure and clamping force for each case using three gates.

	Case 1	Case 2	Case 3	Case 4
P_{max} (Mpa)	18.58	20.93	18.59	19.04
F_{clamp} (kN)	1172.01	1222.46	1168.87	1185.81

Table 6 Maximum pressure and clamping force depending on gate design.

	Number of gates	P_{max} (MPa)	F_{clamp} (kN)
A	1	28.45	1070.95
B	2	28.89	1366.36
C	3	20.93	1222.46
D	3	18.59	1168.87

Table 6 summarizes the maximum pressure and clamping force depending on gate designs. Here, A is the case 3 using a single gate, B the case 1 using two gates, and C and D cases 2 and 3 using three gates.

From these results, it can be seen that the use of more gates usually reduced the maximum pressure and clamping force. This was because as the number of gates increased the volume to be filled by each gate decreased. Also the required clamping force became lower as the maximum pressure was lower. However, the decrease ratio of clamping force was smaller than that of maximum pressure. This was because the area with high pressure increased although the maximum pressure decreased.

For a final decision, therefore, the runner system and various constraints of the production system must be considered.

4. Conclusions

The design of gate locations in injection molding of a dashboard for automobiles was carried out with CAMP*mold*, a PC-based simulation system for injection molding. A dummy runner system was developed to make simulations available without actually constructing a runner system. The numbers and locations of gates for the process were varied in the present investigation. In this procedure, the simulation objective was achieved in terms of reducing the maximum pressure and clamping force and removing weld lines. It was verified that the balance of flow is important in reducing molding pressure.

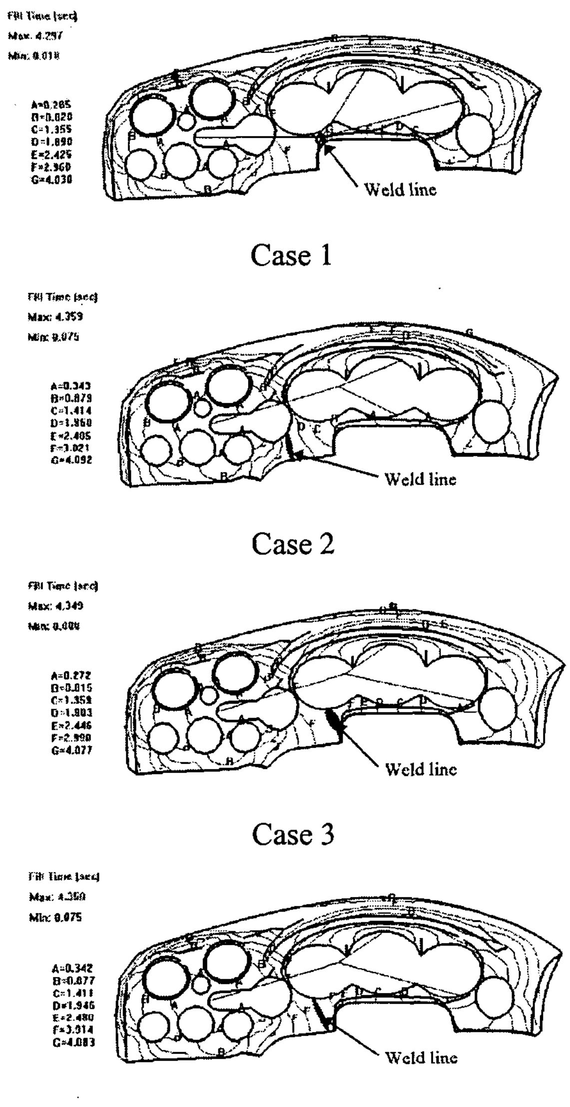

Fig. 9 Filling time distribution and weld line formation for each case using three gates.

References

(1) R. K. Irani, B. H. Kim, and J. R. Dixon, "Towards Automated Design of the Feed

System of Injection Molds by Integrating CAE, Iterative Redesign and Features," Journal of Engineering for Industry, Transactions of the ASME, Vol. 117, No. 1, pp.72-77, 1995.
(2) I. Pandelidis and Q. Zou, "Optimization of Injection Molding Design. Part I: Gate Location Optimization," Polymer Engineering and Science, Vol. 30, No. 15, pp.873-882, 1990.
(3) I. Pandelidis and Q. Zou, "Optimization of Injection Molding Design. Part II: Molding Conditions Optimization," Polymer Engineering and Science, Vol. 30, No. 15, pp.883-892, 1990.
(4) M. Saxena and R. K. Irani, "An Integrated NMT-Based CAE Environment – Part II: Applications to Automated Gating Plan Synthesis for Injection Molding," Engineering with Computers, No. 9, pp.220-230, 1993.
(5) K. H. Han and Y. T. Im, "Compressible Flow Analysis of Filling and Post-Filling In Injection Molding with Phase-Change Effect," Composite Structures, Vol. 38, pp.179-190, 1997.
(6) K. H. Han and Y. T. Im, "Analysis of Filling in Injection Molding with," Transactions of the KSME (A), Vol. 21, No. 5, pp.735-745, 1997.
(7) D. S. Choi and Y. T. Im, "Prediction of Shrinkage and Warpage in Consideration of Residual Stress in Integrated Simulation of Injection Molding," Composite Structures, Vol. 47, pp.655-665, 1999.
(8) K. H. Han and Y. T. Im, "Modified Hybrid Closure Approximation for Prediction of Flow-induced Fiber Orientation," Journal of Rheology, Vol. 43, No. 3, pp.569-589, 1999.
(9) K. H. Han and Y. T. Im, "Effect of Closure Approximation on Fiber Orientation Distribution in Injection Molding," International Journal of Forming Processes, Vol. 3, No. 3-4, pp.213-234, 2000.
(10) K. H. Han and Y. T. Im, "Numerical Simulation of Three Dimensional Fiber Orientation in Injection Molding Including Fountain Flow Effect," Polymer Composites, Vol. 23, No. 2, pp.222-238, 2002.
(11) CAMP*mold* v1.0 users manual, http://camp.kaist.ac.kr/campseries, 2000.
(12) A. I. Isayev, "Injection and Compression Molding Fundamentals," Marcel Dekker, New York, 1987
(13) H. H. Chiang, C. A. Hieber, and K. K. Wang, "A Unified Simulation of the Filling and Postfilling Stages in Injection Molding. Part I: Formulation," Polymer Engineering Science, Vol. 31, pp.116-124, 1991.
(14) K. H. Yoon and K. H. Cho, "An Experimental Study on The Removal of Weldline by Moving Core Method," Transactions of the KSME (A), Vol. 24, No. 7, pp.1787-1794, 2000.